



A Compendious Rheo-Mechanical Test for Printability Assessment of 3D Printable Concrete

Seung Cho^(✉), Jacques Kruger, Frederick Bester,
Marchant van den Heever, Algurnon van Rooyen,
and Gideon van Zijl

Division for Structural Engineering and Civil Engineering Informatics,
Stellenbosch University, Stellenbosch 7600, South Africa
scho@sun.ac.za

Abstract. A successful 3D concrete print (3DCP) is controlled by a sound buildability and good pumpability. Since both factors rely on the behavior of concrete in the fresh state, rheological assessment is crucial prior to 3DCP. In a previous study done by Roussel [1], a correlation of numerical simulation of ASTM mini-slump cone flow and rheometer results was successfully addressed. As the model solely considers material flow under gravitational loading, this model can be adjusted with an external source of energy in the form of impact loading by vertical drop from a certain height to emulate the agitation and deposition process of 3DCP. A flow table and rheometer tests were executed with 5 samples of different consistency. Consecutively, 3DCP validation was performed except for the sample with no superplasticizer content. The study shows the relative deformation (%) varied in a range of 34% - 89% after the drops according to the consistency of the sample. The initial static and dynamic yield stresses are also presented in a range of 0.94–6.82 kPa and 0.54–4.73 kPa respectively. Based on the results, flow table reading ranges are suggested for suitable 3D printability.

Keywords: 3D concrete printing · Rheo-Mechanics · Printability test method · Mini-slump cone · Buildability · Rheology

1 Introduction

The quality of an extrusion and layer depository based digital construction, so-called 3D concrete print (3DCP), is influenced by several factors, e.g. printing parameters, the geometry of printed object, and rheological properties of the material in the fresh state. Buildability, extrudability and pumpability are the terms to describe the printability or quality of the 3D printing. To manipulate the printability, the rheology of material is the dominant variant while the others are normally considered as prescribed factors. Hence, the correctly measured rheological measurement data is significantly important to design 3D printable concrete material.

Sophisticated rheological measurement devices, known as rheometers, are customarily employed to characterise rheological behaviour due to its comprehensiveness.

From the results the static and dynamic yield shear stresses are plotted to attain thixotropic parameters, which are among the principal factors to determine printability of the material [2, 3]. Due to the rather lengthy process and intricate procedure, the rheological characterisation is commonly performed on separate batches of concrete before commencing with the 3D printing process. Due to the complex process as well as the high-cost measurement devices, it is mainly used in a laboratory environment. A further complication is variability in rheology properties in different batches despite care for reproducibility [4].

Despite the existing compact test methods for measuring specific yield stress, e.g. continuous penetration test [5], there is a possibility to adapt the ASTM mini-slump cone test [6] for 3D printing because it is relatively quick and simple, but comprehensive. Roussel et al. [7] developed a numerical model for the ASTM mini-slump cone flow when the mold is solely lifted. Here it is proposed to evaluate printability by including a mechanical impact loading caused by dropping the top plate by a certain height. The impact loading may simulate the agitation induced by pumping and transport of the concrete before extrusion during 3DCP. Consequently, an indication of microstructural breakdown resulting in the reduced dynamic yield shear stress can be obtained, by which pumpability and buildability could be estimated concurrently.

This is a preliminary experimental study to investigate the correlation between rheological measurements obtained by a rheometer and the spread diameter from flow table testing after applying impact loadings.

2 Experimental Methods and Program

2.1 Mix Design and Test Set Configuration

A suitable mix design for 3DCP, given in Table 1, has been developed with locally sourced materials and optimised in previous studies [8], consequently forming the reference mix (S_1SP) for this research.

Table 1. 3D printable concrete mix composition.

Constituent	Description	RD	Mass [kg]
Cement	PPC SureTech 52.5 N	3.14	579
Fly ash	DuraPozz Class F	2.2	165
Silica fume	SiliconSmelters MicroFume	2.1	83
Fine aggregate	Local Malmesbury (4.75 mm max. size)	2.65	1167
Water	Potable Tap Water	1	261
SP	Chryso Premia 310	1.05	5.0

In order to characterise the behaviour of fresh concrete under impact loading on a flow table, the consistency of fresh concrete was differentiated into 5 test sets with altered polycarboxylate polymer-based superplasticizer (SP) contents. From the reference or Standard sample mix (S_1SP), two low consistency samples were prepared with a superplasticizer content reduction by 50% and 100%, namely S_0.5SP and

S_0SP respectively, while the other samples contain increased superplasticizer by 50% and 100%, namely S_1.5SP and S_2SP respectively, to achieve a high consistency (see Table 2). On average, the density of freshly mixed concrete mixture is 2100 kg/m^3 .

Table 2. Test set configurations.

	S_0SP	S_0.5SP	S_1SP	S_1.5SP	S_2SP
SP contents [kg/m^3]	0 (-100%)	2.5 (-50%)	5 (+0%)	7.5 (+50%)	10 (+100%)

2.2 Slump Cone Flow Table Test

As specified in ASTM C230/230 M, the standardised flow table apparatus was prepared with the presence of recording cameras in three orthogonal directions (i.e. x-(front), z- (side), and y- (top) directions), as shown in Fig. 1.a.

A smooth finished conical bronze or brass mould (50 mm high, top diameter 70 mm and bottom diameter 100 mm) is first placed on the mounted circular rigid flow table with a finely machined plane surface free of defects (255 mm diameter and 4.08 kg mass). Once the mould is filled with a freshly prepared concrete mixture, the mould is gently lifted without a remarkable disturbance. An impact loading is transmitted to the mixture caused by the collision of the top flow table to the bottom stand as it drops through a constant height of 12.7 mm for 15 times at a constant rate (See Fig. 1.a). A frictional intervention between the mould and flow table surface is assumed to be negligible since the contact surface of both apparatuses is smoothly machined.

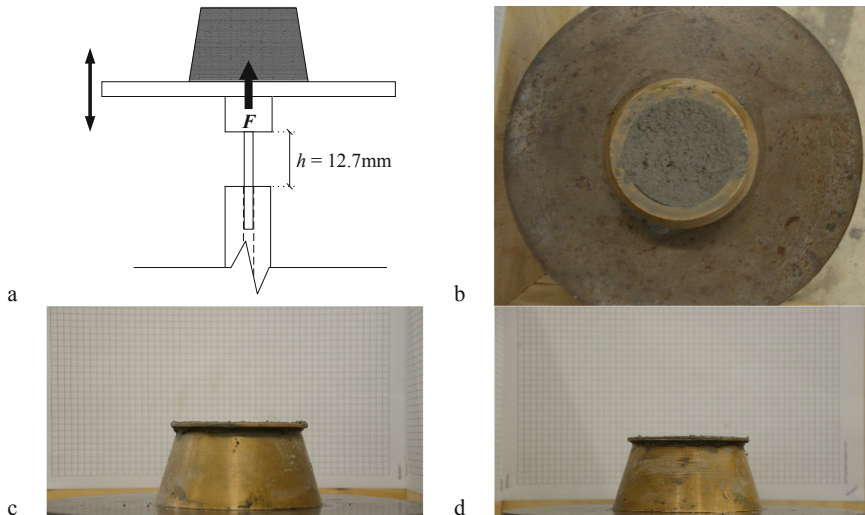


Fig. 1. a. A brief illustration of the impact loading caused by flow table test; b. real setup of slump cone of top view for calibration purpose (along the y-axis); c. front view (along x-axis); d. side view (along z-axis).

Stress induced by applied loading, i.e. self-weight and impact, is depicted as a horizontal line and labelled as C in Fig. 2. The line-C moves downwards when the specimen surface contact area with flow table increases as it spreads, and it moves upwards when impact loading is applied. In other words, deformation starts when the line-C exceeds the shear capacity of a material, until a state of equilibrium is reached again.

The initial deformation (d_0) is solely influenced under the gravitational loading from the density of the concrete mixture when the mould is lifted with no agitation action. Since the material is not disturbed or agitated, the flow onset of d_0 only occurs when line-C by gravitational load exceeds the material's initial static shear capacity (line-A in Fig. 2). The initial deformation ceases when a state of equilibrium is reached, which can also be described as material shape retention.

Likewise, plastic deformation begins when the line-C by first impact loading exceeds line-A. However, the shear stress-responsive curve may be subsided down due to the structural breakdown of material which was displayed as a deformation. Subsequently, the subsided shear static capacity (line-B) becomes the verge for flow onset.

Because the relatively constant time gap between the vertical drops does not allow enough time for significant structural buildup, the line-B is assumed to remain constant.

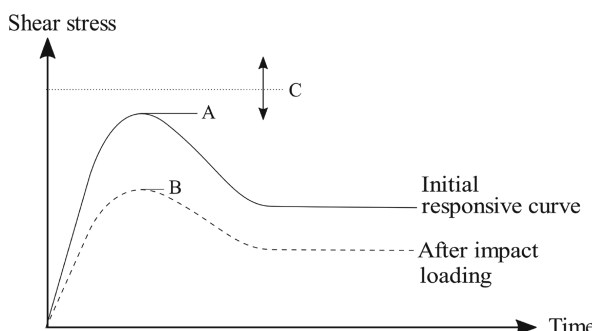


Fig. 2. An illustration of flow onset of a thixotropic concrete mixture, which depends on the loading and material behavior in fresh states.

The average flow diameter of the mixture is then digitally recorded by means of video footage. In processing the digitally recorded image data, the scale is calibrated with the outer diameter of the bronze mould, 105 mm with 5 mm thickness of the mould, for all directions and test sets. Based on the calibration, the relative displacement [%] can be recorded at every drop.

2.3 Rheometer Measurement

The empirical and indicative correlation of rheological parameters with slump flow diameter is the main objective of this paper. Thus, a precise measurement device is required, here a rheometer, to obtain the rheological parameters (static yield stress, τ_s ; dynamic yield stress, τ_d ; structuration rate, A_{thix} [2] and re-flocculation rate, R_{thix} [3]).

A rotational cylinder type rheometer, RHM-3005/3009, produced by the German Instruments ICAR (International Center for Aggregate Research) was used to investigate the rheological parameters. A stress growth test, determining static and dynamic yield stress of the mixture, at 1.0 s^{-1} shear rate was performed at various resting periods, up to 300 s, for time-dependent thixotropic parameters determination. However, it is noted that the test setup with a relatively short resting time frame, designed to emulate the quick nature of the flow table test, does not showcase the long-term thixotropic parameter, the structuration rate, A_{thix} , i.e. no distinct structuration behaviour was shown within 300 s.

2.4 3D printing validation

Once the rheological characterisation process was finished for all test sets, circular column samples were 3D printed with the five different fresh materials as validation. The currently available 3D printer has a 1 m^3 build volume and 25 mm diameter nozzle at three translational degrees of freedom [9].

As the validation is to check the printability performance, i.e. buildability and pumpability, during a sole period of printing, an analytical buildability model presented by Kruger et al. [8] was employed while the pumpability can be checked with a presence of discontinuity of printing filament. The model predicts the number of buildable filament layers during the 3D printing until it fails by plastic yielding failure mechanism which occurs either: 1) during re-flocculation for a fast vertical building rate or 2) during structuration for a normal or slow vertical building rate (see Fig. 3). The buildability model includes the 3D print parameters presented in Table 3 for the selected 250 mm diameter circular hollow column. 3D printing continues until global failure occurs.

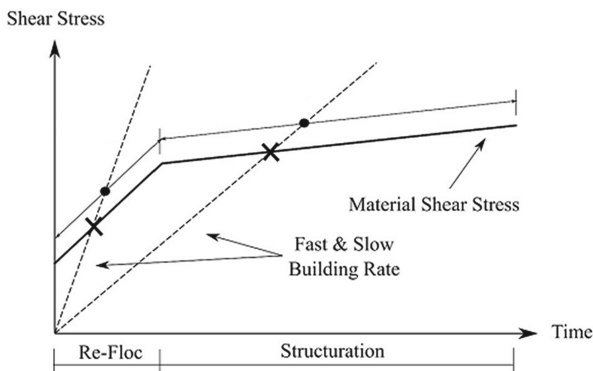


Fig. 3. A time-dependent bi-linear thixotropic model [3] with example building rates. Plastic yielding failure occurs during either re-flocculation or structuration phases depends on the building rate [8].

Table 3. Input parameters for buildability model prediction.

Parameters	Layer height (h)	Layer width (w)	Path length per layer (l)	Printing speed (v)	Aspects ratio (h/w)
Value	10 mm	30 mm	785 mm	60 mm/s	0.33

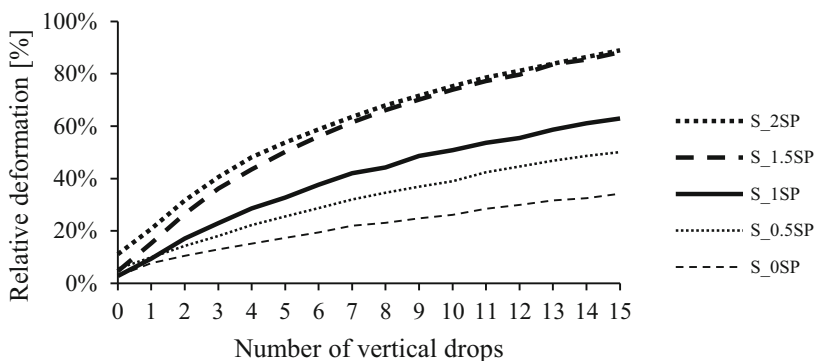
3 Results

3.1 Slump Cone Flow Table Test

The mean value of flow diameter or relative deformation to the 100 mm undeformed diameter in each test set was calculated by recorded digital images in three directions.

The mean flow diameters at each vertical drop (d_1, \dots, d_{15}) for all test sets are plotted in Fig. 4. Only S_2SP displayed a notable initial deformation (d_0) under self-weight loading. Each of S_0SP, S_0.5SP and S_1SP shows its own distinctive deformation profile and approximately linear increments while S_1.5SP and S_2SP result in a similar profile. In other words, the superplasticizer overdosage passes a saturation point in a concrete mixture. Thus, the saturated concrete mixture yields a similar flow response under the loadings even if the dosage is not the same.

Table 4 presents the initial deformation and the final deformation after 15 vertical drops. The correlation between the result and the rheological parameter will be discussed in the following section.

**Fig. 4.** Relative deformation in percentage at each vertical drop for all test sets.**Table 4.** Initial and final mean flow diameter (units are in mm).

	S_0SP	S_0.5SP	S_1SP	S_1.5SP	S_2SP
d_0	102.79	105.61	102.76	104.61	111.15
d_{15}	134.25	150.09	162.90	188.27	188.97
Difference (%)	30.6%	42.1%	58.5%	80.0%	70.0%

3.2 Rheometer Measurement

The initial rheological parameters are crucial to predict the buildability and pumpability. Initial stress growth rheometer test results of all test sets are shown in Fig. 5.a with static and dynamic yield stress values. Considerable static and dynamic yield stress increases are found in the test sets with reduction of superplasticizer content, i.e. S_0SP and S_0.5SP. On the other hand, the control sample, S_1SP, exhibits a similar rheological response to S_1.5SP.

The re-flocculation rate (R_{thix}) calculation plot for the control sample is presented in Fig. 5.b. The graph shows a rapid restoration of its flocculation structure after the initial dynamic yield stress which emulates the agitation process. It is a typical response of thixotropic material where it also displays the best fitting in the graph.

The calculated re-flocculation rate and initial shear yield stress values are summarised in Table 5 as inputs for the buildability prediction model.

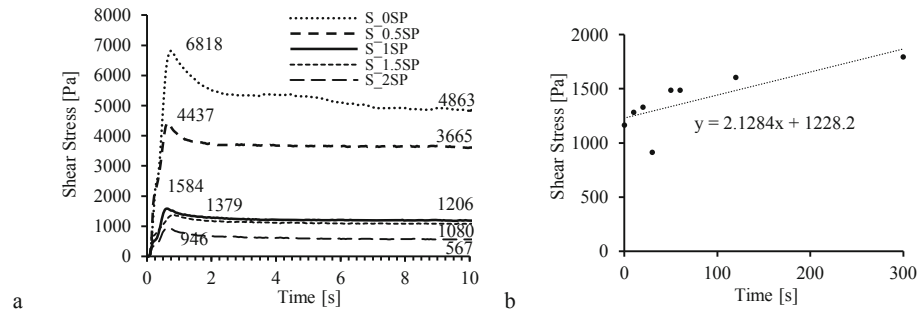


Fig. 5. a. Initial stress growth rheometer test results; b. Calculation of the re-flocculation (R_{thix}) rate of S_1SP.

Table 5. Summarised rheological parameters.

	S_0SP	S_0.5SP	S_1SP	S_1.5SP	S_2SP
τ_s [Pa]	6818	4437	1584	1379	946
τ_d [Pa]	4863	3665	1206	1080	567
R_{thix} [Pa/s]	1.47	1.69	2.13	0.42	0.68

3.3 3D printing validation

The images in Fig. 6 depict the successfully 3D printed column just before the onset of global failure for all samples, i.e. S_0.5SP, ..., S_2SP. As S_0SP exhibited excessively stiff behavior in a fresh state, it was considered not to print with no external agitation energy source, e.g. poker vibrator, due to the possibility of damage in a pump or delivery pipe.

It is noted that a slight stoppage at layer 10 and 20 was found during the printing process for unknown reasons. The lagging motion created an excessive deposit at the point. This phenomenon is discussed in the next section.

Table 6 shows the predicted maximum number of layers for the 3D printed object and the recorded number of layers during the validation process. It is found that none of the validation results exceeds the prediction even though most of the results fall in a reasonable range. Although S_0.5SP recorded the highest number of printed layers, it resulted in the intolerable error to the buildability model prediction. This discrepancy which results in a relatively low number of printed layers despite the high static yield stress will be further investigated.

Table 6. Number of printed layers without a major deformation or global failure (governing thixotropic parameter is specified in the bracket).

	S_0SP	S_0.5SP	S_1SP	S_1.5SP	S_2SP
Predicted layers	113 (A_{thix})	78 (A_{thix})	28 (A_{thix})	20 (R_{thix})	11 (R_{thix})
Validated layers	—	33	26	20	9
Error %	—	-58%	-7%	0%	-18%

With no discontinuity of material delivery from pump to nozzle in printing process for all test sets, S_0.5SP (Fig. 6.a) and S_1SP (Fig. 6.b) exhibit sound buildability while the other two (Fig. 6.c and 6.d) shows a notable local deformation of each filament, consequently it leads layers to be wobbled and exhibit a global deformation of the structure. In aspects of surface finish quality, S_0.5SP shows poor surface finishing in the form of surface rupture due to the low superplasticizer content.

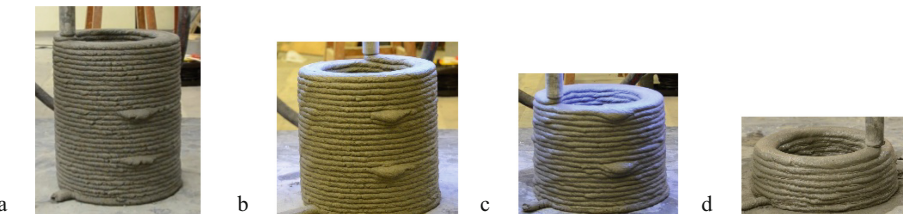


Fig. 6. 3D printing validation of all test sets, except S_0SP which is considered not to be pumpable. a. S_0.5SP; b. S_1SP; c. S_1.5SP and d. S_2SP.

4 Discussion

This experimental study is a preliminary feasibility study for the development of an adjusted analytical model for flow table testing with impact loadings. Since the vertical impact loading of the flow table is a different form of agitation than the rotational agitation of rheometer, a strong correlation is not expected. The small number of

samples together with substantial superplasticizer dosage differences in samples also do not justify a strong conclusion. However, it is worthwhile to find that the repetitive dynamic loading to the material successfully emulates the structural breakdown of the material.

A bi-linear relationship of shear yield capacity over superplasticizer dosage is found. A high rate of shear stress reduction is expected before the saturation point, then the rate flattens out. Likewise, slump flow table results also exhibit a bi-linear relationship (see Fig. 7.a). Even though the intersection bi-linear in two graphs slightly differ, it can be postulated an exact saturation point is in between S_1SP and S_1.5SP.

During the 3D printing process, the percentage of error was relatively small except S_0.5SP which resulted in a significantly lower number of layers than what is predicted. Due to the absence of structuration rate, it is possible to perform worse than the prediction model. Thus, an exact material structuration rate, A_{thix} , is crucial to properly perform the validation test for future study.

Also, geometric imperfections were found at layers 10 and 20 during the printing process which was caused by reduced nozzle speed for unknown reasons. A slight lagging of 3D printer caused an excessive deposit at a point which causes the defects. This factor also contributes towards the poor performance of the material in the 3D printing process.

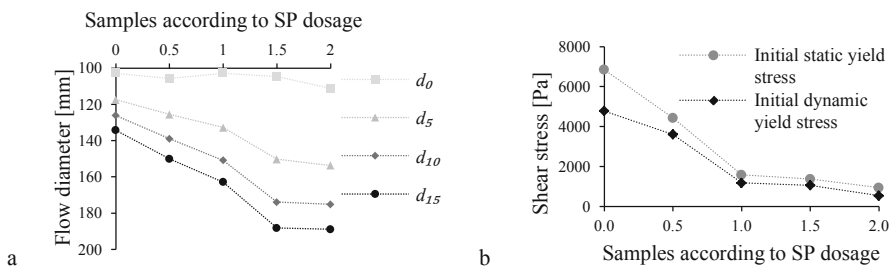


Fig. 7. a. Spread flow diameter at 0, 5, 10 and 15 vertical drops, i.e. d_0 , ..., d_{15} . The horizontal axis represents the test sets, S_0SP to S_2SP (left to right); b. Initial static and dynamic yield stress against test sets with different superplasticizer dosage.

5 Conclusion and Future Works

In this study, an attempt was made to correlate rheological parameters obtained by a sophisticated measuring device and a slump flow table test with impact loading, which has much simpler yet compendious execution. Based on the measured results, a strong and direct correlation between the two measurements is not made, due to a limited number of samples and a remarkable superplasticizer dosage difference.

However, this study can be extended to a quantitative assessment to further investigate an empirical correlation. Ongoing work aims to develop an adjusted analytical model of the mini-slump with the inclusion of impact loading and varying contact area.

From the results above, a suggestion of this indicative parameter, flow table diameter, for 3DCP is proposed in Table 7.

Table 7. 3DCP printability according to the flow table diameter reading ranges of the test results.

Readings [mm]	-130*	130–150	150–165	165–180	180+
Suggestion	×	Δ	○	Δ	×

*This may be printed with a presence of external energy source, e.g. poker vibrator. But, poor quality of 3DCP is expected.

- ×: Not recommended for 3DCP as the material exhibits a drastic fresh behavior of being either overly stiff or flowable.
- Δ: It may be acceptable for 3DCP. However, it may possibly result in a poorly printed object or poor buildability performance.
- ○: It can be acceptable for 3DCP.

References

1. Roussel, N.: Correlation between yield stress and slump: comparison between numerical simulations and concrete rheometers results. *Mater. Struct.* **39**, 501–509 (2006)
2. Roussel, N.: A thixotropy model for fresh fluid concretes: theory, validation and applications. *Cem. Concr. Res.* **36**, 1797–1806 (2006)
3. Kruger, P.J., Zeranka, S., van Zijl, G.P.A.G.: An ab initio approach for thixotropy characterisation of (nanoparticle-infused) 3D printable concrete. *Constr. Build. Mater.* **224**, 372–386 (2019)
4. Kruger, P.J., Cho, S., Zeranka, S., Viljoen, C., van Zijl, G.P.A.G.: 3D concrete printer parameter optimisation for high rate digital construction avoiding plastic collapse. *Compos. Part B: Eng.* **183**, 107660 (2020)
5. Reiter, L., Wangler, T., Roussel, N., Flatt, R.J.: Continuous characterization method for structural build-up. In: 2nd RILEM Conference on Rheology and Processing of Construction Materials (RheoCon2), Dresden (2019)
6. ASTM C230/C230M: Standard specification for flow table for use in tests of hydraulic cement (2014)
7. Roussel, N., Coussot, P.: Fifty-cent rheometer for yield stress measurements: from slump to spreading flow. *J. Rheology* **49**(3), 705–718 (2005)
8. Kruger, P.J., Zeranka, S., van Zijl, G.P.A.G.: 3D concrete printing: a lower bound analytical model for buildability performance quantification. *Autom. Constr.* **106**, 102904 (2019)
9. Cho, S., Kruger, P.J., Zeranka S., van Zijl, G.P.A.G.: 3D printable concrete technology and mechanics. pp. 11–18, *Concrete Beton* (2019)